A Joint Inversion Approach of Capacitive and Resistive Measurements for the Estimation of Water Saturation Profiles in Concrete Structures

Marie Antoinette Alhajj, Géraldine Villain, Sébastien Bourguignon, Sérgio Palma Lopes

A Joint Inversion Approach of Capacitive and Resistive Measurements for the Estimation of Water Saturation Profiles in Concrete Structures

Marie A. Alhajj[1], Géraldine Villain[1], Sébastien Bourguignon[2], Sérgio Palma Lopes[3]

[1] Mast-Lames, Ifsttar, Site de Nantes, Allée des Ponts et Chaussées, Bouguenais Cedex France marie-antoinette.alhajj@ifsttar.fr
geraldine.villain@ifsttar.fr

[2] Centrale Nantes, 1 rue de la Noë, Nantes Cedex 3, France sebastien.bourguignon@ecnantes.fr

[3] Gers-GéoEnd, Ifsttar, Site de Nantes, Allée des Ponts et Chaussées, Bouguenais Cedex France sergio.lopes@ifsttar.fr

XV Durability of Building Materials and Components
20-23 October 2020, Barcelona, Spain

INFORMATION

Keywords:
Durability
Nondestructive Techniques
Capacitive and Resistive Measurements
Inversion Procedure

DOI: 10.23967/dbmc.2020.182

Published: 25/09/2020

XV International Conference on Durability of Building Materials and Components
DBMC 2020, Barcelona
C. Serrat, J.R. Casas and V. Gibert (Eds)

A Joint Inversion Approach of Capacitive and Resistive Measurements for the Estimation of Water Saturation Profiles in Concrete Structures

Marie A. Alhajj[1], Sébastien Bourguignon[2], Sérgio Palma Lopes[3] and Géraldine Villain[1]

[1] Mast-Lames, Ifsttar, Site de Nantes, Allée des Ponts et Chaussées, CS 5004, 44344 Bouguenais Cedex France, marie-antoinette.alhajj@ifsttar.fr, geraldine.villain@ifsttar.fr

[2] Centrale Nantes, 1 rue de la Noë, 44321 Nantes Cedex 3, France, sebastien.bourguignon@ec-nantes.fr

[3] Gers-GéoEnd, Ifsttar, Site de Nantes, Allée des Ponts et Chaussées, CS 5004, 44344 Bouguenais Cedex France, sergio.lopes@ifsttar.fr

Abstract. *Concrete is a construction material that is well known for its durability. However, it is exposed to environmental attacks that lead to the penetration of aggressive agents such as water and chlorides, thus, threatening its durability and service life. Within this context and exploiting the sensitivity of the electromagnetic properties of concrete to its water content, the literature suggests determining water saturation profiles using non-destructive techniques. For instance, measuring the electrical resistivity at several points of the surface of the concrete structure can lead to an estimate of the resistivity depth profile. Then, after a calibration step, the water saturation depth profile can be obtained and the durability can be assessed. Similarly, the water depth profile can be assessed by dielectric permittivity measurements. In this paper, we propose a new inversion scheme based on the combination of both resistive and capacitive measurements: resistivity and permittivity measurements are inverted jointly to estimate the water saturation profile in concrete. Numerical experiments with simulated data show that information gathered from the two measurements enriches the inversion process, leading to the determination of more reliable water saturation profiles.*

Keywords: *Durability, Nondestructive Techniques, Capacitive and Resistive Measurements, Inversion Procedure.*

1 Introduction

Nondestructive (ND) methods are promising to assess the durability of concrete. They are non-intrusive and allow continuous structure monitoring (Balayssac, 2017). This study focuses on estimating the concrete saturation degree and handles two kinds of measurements: the DC-electrical resistivity and the dielectric permittivity. Both quantities are sensitive to the water content in concrete, and in a complementary way (Fares, 2018), and can, therefore, be used to evaluate the durability of concrete towards water ingress (Balayssac, 2017). The method consists of performing resistivity and permittivity measurements at the surface of the structure; then, an inversion procedure is required to retrieve the electromagnetic depth profiles. Finally, water saturation is obtained through calibration of the electromagnetic properties.

The inversion of measurements has been performed using either the resistivity or the permittivity data to obtain the water saturation with depth profile (Fares, 2016). However, inversion results may lack reliability, in particular, due to the small number of available data, the presence of noise in the measurements, and the lack of sensitivity of each data set to the

water saturation profile. Therefore, a possible solution to improve the inversion of ND measurements relies upon combining the two types of data, the electrical resistivity, and the dielectric permittivity, taking advantage of their complementarity (Tathed, 2018).

In Section 2, we introduce a brief description of both ND methods. Then, in Section 3, the searched saturation profile is modeled with a parametric curve, and both the forward model and the inverse problem are discussed. Our joint inversion procedure is described in Section 4. Finally, Section 5 presents numerical simulations evaluating the performance of the proposed methodology.

2 Electromagnetic Properties of Concrete

2.1 DC-Electrical Resistivity

The DC-electrical resistivity of concrete, noted ρ [Ω.m], expresses the ability of the material to oppose the flow of free electric charges when it is subjected to an electric field. In a homogeneous and isotropic material, it is expressed by the Ohm's law ratio of the measured voltage drop V [V] to the applied current intensity I [A], multiplied by a geometric factor G_r [m] :

$$\rho_a = G_r \frac{V}{I}. \tag{1}$$

The resistivity measurement principle consists of transmitting a direct current (DC) into the concrete using two electrodes and measuring the induced potential drops between one or several pairs of electrodes. Then, the 'apparent' resistivity can be calculated using Eq. (1). Since concrete is usually not a homogeneous material, the latter observable is not the 'true' resistivity of concrete but rather an integrating value over a volume depending on the electrode array configuration and size (Loke, 2004) (Presuel-Moreno, 2010) .

In this study, two electrode configurations are considered to measure apparent resistivities, the Wenner and the Schlumberger arrays (Loke, 2004). Our measuring device consists of a multi-electrode resistivity probe formed by 14-point electrodes equally spaced every 20 mm (Du Plooy, 2013). For all possible electrode combinations following the Wenner and Schlumberger configurations, a dataset consisting of about 100 apparent resistivities can be obtained.

2.2 Dielectric Permittivity

The dielectric permittivity, noted ε [F/m], is related to the phenomenon of electric polarization which results from the relative displacement of the bound charges in the material under the action of an external electric field. Due to the energy losses that accompany the polarization phenomenon, the permittivity can be expressed using a complex variable where the real part is the ability of the material to store electric energy. Consequently, the relative dielectric permittivity of concrete, ε (dimensionless), can be obtained from the system's capacitance, C [F], the vacuum permittivity, ε_0 [F/m] and the geometric factor, G_c [m]:

$$C = G_c . \varepsilon_0 . \varepsilon. \tag{2}$$

The measurement principle consists in applying an alternating current between two or more electrodes placed on the surface of the sample and measuring the resonance frequency of the

electrode-concrete system. The measuring device and consists of four different types of probes, each composed of metal plate electrodes and Plexiglas® support. The probes differ by their number of metal plates, their dimensions and the spacing between them (Fares 2016):

- electrode GE consisting of 2 plates (70xx40 mm^2) with a plate spacing of 40 mm,
- electrode ME+ consisting of 3 plates (70x15 mm^2) with a plate spacing of 15 mm,
- electrode ME consisting of 4 plates (70x10 mm^2) with a plate spacing of 10 mm,
- electrode PE consisting of 5 plates (70x5 mm^2) with a plate spacing of 5 mm.

Using this device, four apparent permittivity values can be collected for each measuring sequence, whose depth sensitivity increases with both the size and the spacing of the electrodes. Note that the measured apparent permittivity is equal to the 'true' permittivity of concrete in case of a semi-infinite homogeneous medium. Nonetheless, when the medium is of finite dimensions or is not homogeneous, the measured apparent permittivities must enter an inversion procedure to obtain the true permittivity distribution in the concrete medium.

3 Saturation Profile

In this section, a definition of the saturation degree is provided as well as the saturation profile chosen for this study. Then, the methodology for computing the forward model and solving the inverse problem for each ND electromagnetic method is briefly explained. Finally, our joint inversion approach is presented.

3.1 Definition

The saturation degree, noted S, represents the fraction occupied by water in the total pore volume. The saturation degree conditions the penetration of aggressive agents. For this, the determination of the saturation degree makes it possible to predict the degradation of concrete. Moreover, it is important to note that both resistive and capacitive properties of concrete are sensitive to saturation (Balayssac, 2017). The calibration of each of ρ and ε as functions of S is performed on the test specimen. The calibration of the electrical resistivity can be expressed by the model:

$$\rho = AS^{-B} \tag{3}$$

where A and B depend on the concrete specimen studied. Eq. (3) is consistent with Archie's empirical law (1942) proposed by geologists in the oil prospecting field for non-clayey rocks, and then for porous materials such as concrete (Fares, 2018). The calibration of the dielectric permittivity results is performed under the model (Fares, 2018):

$$\varepsilon = aS + b \tag{4}$$

where a and b depend also on the concrete specimen tested. This study aims to deal with the phenomena of drying and soaking in concrete, considered here as non-cyclic and unidirectional. As a result, the degree of saturation in concrete is assumed to evolve only in one direction, which is the depth z perpendicular to the concrete surface, and from a drier state to a wetter state or vice versa (monotonic curve). In addition to that, to better constrain the profile reconstruction, a parametric model is considered using a Weibull curve with the following expression:

$$S(z) = (\theta_1 - \theta_2)\exp(-(\frac{z}{\theta_3})^{\theta_4}) + \theta_2, \quad (5)$$

where θ_1 is the saturation ratio on the surface, θ_2 is the saturation ratio in the structure depth, θ_3 is the scale factor, and θ_4 is the shape factor. Eq. (5) provides a continuous parametric model, where the unknown saturation profile is expressed by the continuous function *S(z)* depending on the four parameters θ_i, i=1, …, 4. The inversion procedure then amounts to estimating the parameters θ_i from the apparent resistivities ρ_a or the apparent permittivities ε_a.

3.2 Forward Model

The forward model consists in the computation of the apparent observables corresponding to a given saturation profile *S(z)*. It has been implemented numerically using the commercial finite element (FE) modeling software COMSOL Multiphysics® (v.5.4). The 3D-concrete model is defined: geometry (700x900x150 mm^3 concrete block), FE mesh, electrode positions for both electrical and dielectric problems (Fig. 1). The FE mesh is finer near the electrodes with a maximum element size of 1 mm and coarser elsewhere with a maximum element size of 5 mm and consists of about 30000 elements. Then, the saturation profile is defined by the Weibull curve defined by Eq. (5). The electrode systems described in Section 2 are used for the measurement simulations.

For the DC-electric problem, 14-point electrodes (see Fig. 1a) represent the multi-electrode resistivity probe. Knowing the saturation profile in concrete depth, the imposed resistivity depth profile is obtained using Eq. (3). Then, the forward model resolution leads to the computation of the apparent resistivities using Eq. (1). For this, the module AC/DC - electric currents of COMSOL is used and positive current is injected in one electrode, negative current in another and an electric potential is simulated in the remaining electrodes. For the dielectric problem, the dielectric plates are represented by surface plates with an infinitely small thickness (Fig. 1b). Knowing the saturation depth profile in concrete, the corresponding permittivity depth profile is obtained using Eq. (4). Then, the forward model resolution leads to the computation of the apparent permittivities using Eq. (2) for each electrode set. For this, the module AC/DC - electrostatics of COMSOL is used and a potential difference is imposed on the electrode plates. For both DC-electric and dielectric models, the following conditions are considered: current conservation within the concrete block, electric insulation of the block boundaries and a null initial potential in the block.

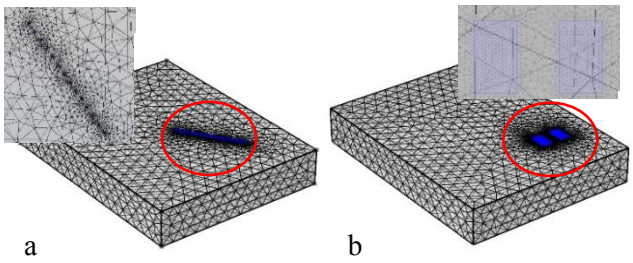

Figure 1. The meshing of the 3D model of a concrete slab (700x900x150 mm^3) with a) the resistivity probe and b) the capacitive electrodes.

3.3 Inverse Problem

The inversion procedure aims to retrieve the water saturation profile from the apparent measurements. This can be achieved by finding the parameters θ in Eq. (5) that best fit the data, by minimizing the least-squares mismatch between the measurements, say d_{mes}, and their prediction corresponding to a given saturation profile, say d_{mod}:

$$\psi = \sum_i (d_{mod_i} - d_{mes_i})^2 \tag{6}$$

In this work, we choose the Levenberg-Marquardt algorithm (Morrison, 1960), which is a standard method for non-linear least-squares optimization problems.

3.3.1 Separate inversion

In previous studies, apparent capacitive and resistive measurements were inverted separately to estimate the water profiles in concrete (Fares, 2016). A single type of measurement was considered (either the resistive or the capacitive ones) to estimate the saturation profile with depth. The method is similar for both types of measurements and is shown in Fig. 2. The goal is to minimize the cost function in Eq. (6), where:

$d_{mod} = \rho_{a_{mod}}$ and $d_{mes} = \rho_{a_{mes}}$ in the inversion of apparent resistivities,

$d_{mod} = \varepsilon_{a_{mod}}$, and $d_{mes} = \varepsilon_{a_{mes}}$ in the inversion of apparent permittivities.

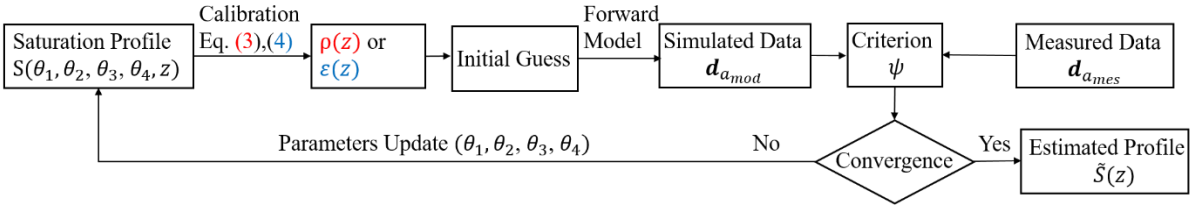

Figure 2. Scheme for the estimation of the saturation depth profile (parameters θ_i) from apparent resistivity or permittivity measurements.

3.3.2 Joint inversion

In this section, we consider a joint inversion approach. The calibration laws established by experimental studies (Eq. (3) and (4)) make it possible to connect each of the properties, electrical resistivity, and dielectric permittivity, to common property, the saturation degree. The joint inversion procedure is presented in Fig. 3. It is an iterative process, which starts with an initial saturation profile given by the initial parameters. Then the resistivity profile is obtained using Eq. (3) and the permittivity profile using Eq. (4). Afterward, the simulated data, that is, the apparent resistivities and permittivities, are computed and compared to the measured data in the joint least-squares criterion given in Eq. (7) ψ, where W_ρ and W_ε are weight parameters given to capacitive and resistive data respectively depending on the quality of these measurements.

$$\psi = W_\rho \sum_i (\rho_{a_{mod_i}} - \rho_{a_{mes_i}})^2 + W_\varepsilon \sum_j (\varepsilon_{a_{mod_j}} - \varepsilon_{a_{mes_j}})^2 \tag{7}$$

The main advantage of the joint inversion is that both measurements are sensitive to

saturation but in a complementary manner. Therefore, the information gathered may yield a better estimation of the saturation profile. Also, the joint inversion could have another advantage concerning the investigation depth of the measurements. Previous studies show that knowing the spacing between electrodes, the investigation depth of the corresponding measurements can be estimated (Loke, 2004) (Fares, 2016). The two ND methods sample differently the investigated volume concerning concrete slab thickness, therefore, combining the two methods makes it possible to better constrain the problem by information on the different regions of this volume of interest.

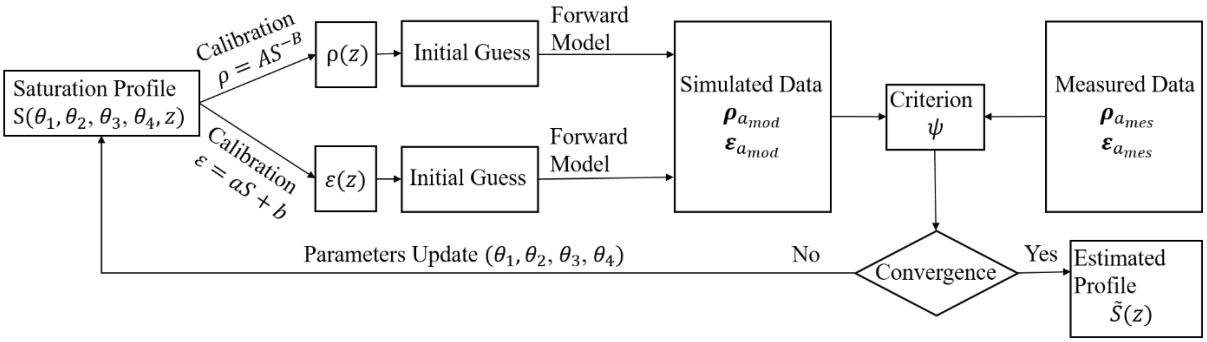

Figure 3. The joint inversion scheme to determine concrete saturation distribution in depth.

4 Numerical Experiments

In this section, numerical experiments are performed to validate the proposed joint inversion approach. Synthetic data are computed, where a saturation profile is generated according to Eq. (5) and represents the 'true' saturation profile (Table 1, column 1). The forward model is computed using the same numerical slab model and electrode simulation as presented in Section 3.2. In all simulations, the initial saturation profile in the optimization procedure is chosen such that the relative error compared to the true profile is equal to 10% (Table 1, column 2).

In the first numerical experiment, we consider noise-free data. The inversion procedure is run successively by considering only apparent resistivity data, only apparent permittivity data, and finally both data sets. The results are shown in Fig. 4. Profiles corresponding to the successive iterations of the Levenberg-Marquardt procedure are represented by the green curves. It is clear that the three inversion methods correctly converge toward the true profile. This result confirms that apparent resistivity and permittivity data, employing their corresponding calibration curves (Eq. (3) and Eq. (4)), can be jointly inverted into a unique saturation profile. In addition to that, the variability of the fitted profile between iterations is important in the inversion of apparent permittivity data (Fig. 4b); due to the smaller number of data, which is equal to the number of unknowns to be determined (the four parameters of the Weibull curve). This variability seems to disappear in the joint inversion (Fig. 4c) due to the additional number of resistivity data added to the permittivity data, which induces a faster convergence to the 'true' profile and a smaller number of iterations (15 for the joint inversion compared to 37 for the permittivity inversion alone). Note that inversion is stopped when the four following criteria are satisfied: the criterion ψ is less than 10^{-6}, the relative variation of estimated parameters between two consecutive iterations is less than 10^{-6}, the number of iterations is higher than 50 and the criterion gradient is less than 10^{-3}.

The second inversion test aims to study the influence of noise in the inversion. Referring to previous noise assessment studies done in the laboratory for capacitive and resistive data (Du Plooy, 2013), three additional sets of computations are carried out. The first one considers noisy resistivity data, such that the coefficient of variation (CV_r defined as the ratio between the standard deviation and the mean of the measurement) is 4%, and permittivity data remain noise-free. The second one considers noisy permittivity data, such that CV_p =2%, and noise-free resistivity data. Finally, the third data set considers noise on both resistivity and permittivity data (CV_r=4% and CV_p=2%, respectively). The results of this study are shown in Table 1, where the estimated profile parameters are given. For each test case, individual and joint inversions are performed. The relative error between the true profile parameters and the estimated one as well as the iteration number is given. In the first study, the two inversions have the same iteration number. However, the relative error is smaller for the joint inversion. For the second study, both the number of iterations and the relative error decrease significantly when the joint inversion is performed. Finally, in the last study, the relative error and the iteration number are the lowest for the joint inversion.

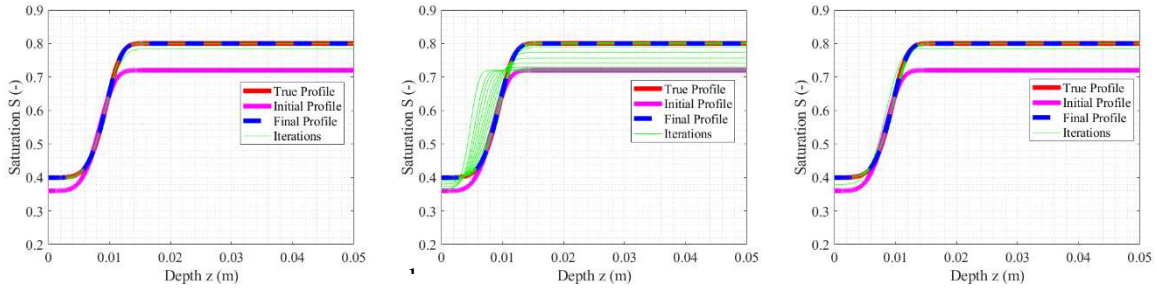

Figure 4. a) Inversion procedure using apparent resistivity data alone –b) Inversion of apparent permittivity data alone and c) Joint inversion of apparent resistivity and permittivity data.

Table 1. Separate and joint inversion results for noisy resistivity and permittivity data.

'True' Profile	Initial Profile	Noise Conditions	Resistivity	Permittivity	Joint
$\begin{bmatrix}0.4\\0.8\\0.01\\5\end{bmatrix}$	$\begin{bmatrix}0.36\\0.72\\0.009\\4.5\end{bmatrix}$	$CV_r = 4\%$ $CV_p = 0\%$	$\begin{bmatrix}0.3927\\0.8006\\0.0101\\4.4996\end{bmatrix}$		$\begin{bmatrix}0.4001\\0.8003\\0.0103\\5.1200\end{bmatrix}$
		Iteration Number	9	9	
		Relative Error	3.21 %	1.26%	
$\begin{bmatrix}0.4\\0.8\\0.01\\5\end{bmatrix}$	$\begin{bmatrix}0.36\\0.72\\0.009\\4.5\end{bmatrix}$	$CV_r = 0\%$ $CV_p = 2\%$		$\begin{bmatrix}0.4031\\0.9500\\0.0119\\10.85\end{bmatrix}$	$\begin{bmatrix}0.4030\\0.8000\\0.0100\\5.4910\end{bmatrix}$
		Iteration Number	50	9	
		Relative Error	38%	2.63%	
$\begin{bmatrix}0.4\\0.8\\0.01\\5\end{bmatrix}$	$\begin{bmatrix}0.36\\0.72\\0.009\\4.5\end{bmatrix}$	$CV_r = 4\%$ $CV_p = 2\%$	$\begin{bmatrix}0.3927\\0.8006\\0.0101\\4.4996\end{bmatrix}$	$\begin{bmatrix}0.4031\\0.9500\\0.0119\\10.85\end{bmatrix}$	$\begin{bmatrix}0.3991\\0.7967\\0.0100\\4.9811\end{bmatrix}$
		Iteration Number	9	50	6
		Relative Error	3.21%	38%	0.25%

5 Conclusion

In this study, we developed a new joint inversion approach for resistivity and permittivity data in concrete structures. Numerical experiments were carried out using synthetic data that showed that the joint inversion of DC-resistivity and dielectric permittivity data can produce a more accurate solution. Simulations using noise-free synthetic data showed good convergence to the 'true' considered saturation profile. Besides, when performing the inversion of synthetic noisy data, the profile estimation is improved by carrying out joint inversion as the relative error between the true and estimated parameters decreases as well as the iteration number compared to the separate inversions. For a complete validation of the joint inversion approach, more intensive simulation tests are required. Afterward, real lab data will be acquired to take into account furthermore the presence of noisy data and to validate the joint inversion approach.

ORCID

Marie Antoinette Alhajj: 0000-0001-7711-5103

References

Balayssac, J.-P. and Garnier, V. (2017). *Non-destructive Testing and Evaluation of Civil Engineering Structures,* Elsevier Press Ltd., London.

Du Plooy, R., Palma Lopes S. and Villain, G. et al. (2013). *Development of a multi-ring resistivity cell and multi-electrode resistivity probe for investigation of cover concrete condition.* NDT&E International.54:27-36.

Fares, M. and Fargier, Y. et al. (2016). *Determining the permittivity profile inside reinforced concrete using capacitive probes,* NDT&E Int. 79:150–161.

Fares, M. and Villain, G et al. (2018). *Determining chloride content profiles in concrete using a resistivity probe*, Cement and Concrete Composites. 94:315-326

Loke, M.H. (2004). *Tutorial: 2-D and 3-D electrical imaging surveys*.

Morrison, D. (1960). *Methods for nonlinear least-squares problems and convergence proofs*. Proceedings of the Jet Propulsion Laboratory Seminar on Tracking Programs and Orbit Determination: 1–9.

Presuel-Moreno, F. et al., (2010). *Characterization of New and Old Concrete Structures Using Surface Resistivity Measurements*, Florida, Florida Department of Transportation Research Center, p. 279.

Tathed, P. Han, Y. and Misra, S. (2018). *Hydrocarbon saturation in Bakken Petroleum System based on joint inversion of resistivity and dielectric dispersion logs,* Fuel 233 (2018) 45–55.